Int. J. Electrochem. Sci., **13 (2018)** 11432 – 11442, doi: 10.20964/2018.12.01

International Journal of
ELECTROCHEMICAL
SCIENCE
www.electrochemsci.org

Modeling the Convective Noise in an Electrochemical Motion Transducer

Vadim M. Agafonov

Moscow Institute of Physics and Technology, Institutsky Lane 9, Dolgoprudny, Moscow Region, 141700.
*E-mail: agvadim@yandex.ru

Received: 5 November 2017 / *Accepted:* 27 April 2018 / *Published:* 5 November 2018

This paper studies the convective noise generated in transducers found in electrochemical motion sensors. The theoretical model uses a Langevin method applied to equations of hydrodynamics. The proposed approach was applied to a transducer with a planar geometry composed of four small electrodes deposited on the walls of the thin channel of the transductive element. For realistic parameters, the modelling results agree well with the experimental data.

Keywords: Ion transport, convective diffusion, sensors, self-noise, hydrodynamics.

1. INTRODUCTION

Progress in electrochemical motion sensing technology over the last 10 years has resulted in the emergence of a new class of highly sensitive sensors, such as short-period and broadband seismometers, seismic accelerometers and angular-motion sensors [1], [2], [3], [4], [5]. The key component in these electrochemical motion sensors is a four-electrode electrochemical cell immersed in a liquid electrolyte for use as a signal converting element [6], [7], [8], [9]. Device operation is based on the fact that an inertial force generates electrolyte flow near the electrodes. In turn, the hydrodynamic flow influences transport of the electrolyte component and, consequently, the inter-electrode electrical current. The variation in the electrical current is readout from the sensor output.

The expansion of practical applications is hampered by the fact that some of the problems associated with the fundamental nature of the processes occurring in the converting elements of electrochemical sensors remain unsolved, which limits possible improvements to their technical parameters. These problems include identification of the nature of self-noise in electrochemical sensors.

The nature of self-noise in electrochemical sensors is complex: it is conditioned by the combined action of a number of physical mechanisms [8], [10]. According to the most recent studies, the main contributors to sensor self-noise are thermohydrodynamic self-noise[11], convective noise[12], geometry noise[8] and noise due to signal conditioning electronics[13].

Some of the above-mentioned mechanisms, such as thermohydrodynamic self-noise and noise due to signal conditioning electronics, are universal for different sensor types and have been previously studied in detail [14]. Other sources of noise are specific to electrochemical sensors, including convective noise, which limits the resolution of the sensor over a wide frequency range [13], [15], [16]. Moreover, convective noise is associated with the fundamental properties of the signal converting element. As a result, understanding and accurately modelling convective type noise is particularly important for realizing further sensor improvements. Currently, only experimental studies for this type of noise have been published [12], with a limited understanding of the physical processes responsible for the generation of convective noise as well as a lack of theoretical models.

The theoretical studies carried out in this work are based on the hypothesis that the output current self-noise for the electrochemical transducer, which has been experimentally studied previously in [12] and named convective noise, is conditioned by the stochastic hydrodynamic flow in the working fluid solution.

2. THEORY

A number of electrochemical transducer configurations have been described in the literature [17], [18], [19], [20]. All of the reported designs comprise two pairs of microelectrodes placed in the channel so that for any direction of inertial force the liquid moves from anode to cathode in one pair of electrodes and from cathode to anode in the other pair. The working solution is a highly concentrated aqueous iodide salt solution (usually potassium iodide) with a small amount of molecular iodine. In the aqueous solution, iodide salt dissolves into positive K^+ and negative I^-ions. Iodine I_2 is present in the form of tri-iodide ions I_3^-. If a voltage is applied between the electrodes, the following reversible electrochemical reaction takes place on the electrodes:

$$3I^- \leftrightarrows I_3^- + 2e \tag{1}$$

The reaction proceeds from left to right on the anode and in the opposite direction on the cathode. Each elementary reaction is associated with the transfer of two electrons across the electrode surface. Thus, the electrical current can be determined if the flow of tri-iodide ions across the electrode is known. This fact is used in a convective diffusion-based model of charge transfer enabling one to consider the transfer of only one type of ion, I_3^-, thus, simplifying the mathematical problem. I_3^- are referred to as active ions. Transport of tri-iodide ions without electric migration is described by the convective-diffusion equation:

$$\frac{\partial c}{\partial t} + D\Delta c = (\vec{v}, \nabla c) \tag{2}$$

where c denotes the I_3^- ion concentration and D denotes the diffusion coefficient.

The hydrodynamic velocity $\vec{v}$ is determined by the Navier-Stokes equation for a non-compressible liquid:

$$\frac{\partial \vec{v}}{\partial t} = \gamma \Delta \vec{v} - \frac{\nabla p}{\rho} + \vec{f}$$
$$div\, \vec{v} = 0 \qquad (3)$$

where γ is viscosity, p is pressure, and $\vec{f}$ is the external volumetric force.

Typically, the boundary conditions on the channel surfaces are a zero hydrodynamic velocity with the following conditions for the active component concentration:

$$\nabla c \cdot \boldsymbol{n}|_{x \notin anode, cathode} = 0$$
$$c|_{x \in anode} = c_a \qquad (4)$$
$$c|_{x \in cathode} = 0$$

The first equation expresses the impermeability condition of the dielectric surface. The second equation expresses the condition of the limiting current at the cathodes. The third equation expresses the assumption of a constant concentration of the active component at the anodes, which, although not completely justified, is often used in calculations to simplify the mathematical model. The applicability of this condition was discussed in a number of previously published papers [21], [22], [23]. It has been found that significant differences are observed in investigations of anode currents compared to more complex boundary conditions that take into account the kinetics of the electrode reactions, as well as for the study of cathodic currents at significant fluid velocities. In this study, we are only interested in cathodic currents, with the analysis limited to low fluid velocities typical for hydrodynamic fluctuations, which allows the use of the simplified boundary condition (4).

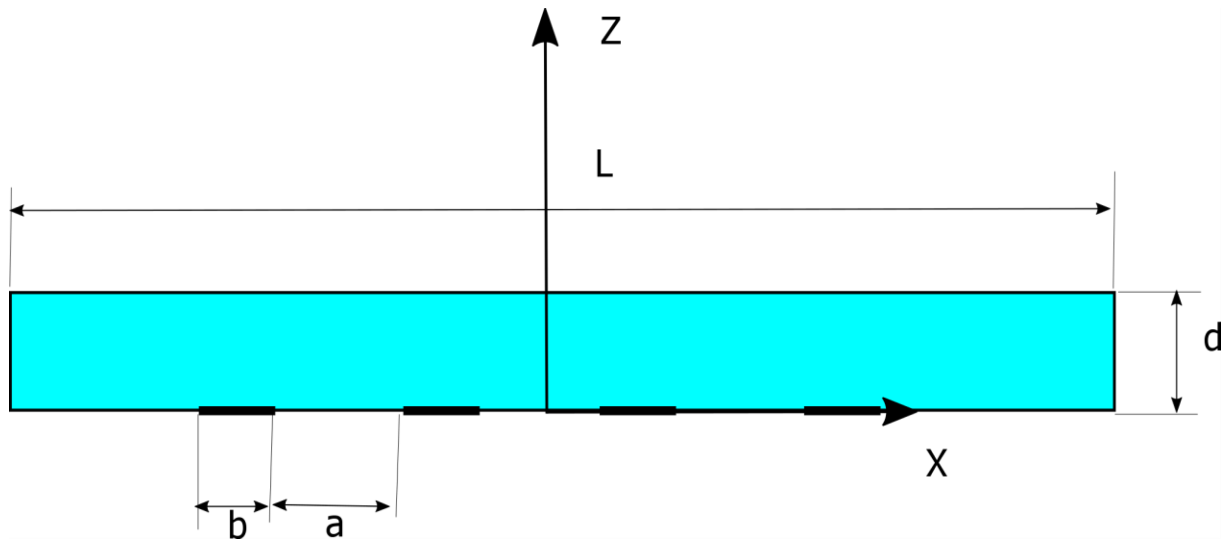

Figure 1. Planar MET cell schematic.

v_z To specify a mathematical model, consider a thin plane channel with four electrodes deposited on one of the channel walls. We introduce a coordinate system with its origin on the surface containing the electrodes, as shown in Figure 1. Both the anodes and cathodes have the same width b and are separated by a distance $2a$. d denotes the thickness of the channel. We assume that the channel thickness d is small compared to the channel length L and width s. Under this condition, as shown in [24], [25], for random hydrodynamic flows, the tangential components of the hydrodynamic velocities v_x, v_y are significantly larger compared to the normal component v_z.The Navier-Stokes equation for the tangential component v_x can be written in the form:

$$\gamma \frac{\partial^2 v_x}{\partial z^2} = f(x,y,z) - \frac{1}{\rho}\frac{\partial P}{\partial x} \tag{5}$$

Место для формулы.

Then, $f(x,y,z)$ is a random volumetric force acting on the liquid, P denotes the local pressure, which changes due to stochastic variations in $f(x,y,z)$, while maintaining validity for the continuity equation:

$$\frac{\partial v_x}{\partial x} + \frac{\partial v_y}{\partial y} = 0 \tag{6}$$

The boundary conditions are a no-slip condition on the solid surfaces and a constant pressure condition $P(x,y,z)|_{\pm l/2} = const$ on the ends of the channel. Note that the latter limitation does not influence the possibility of the pressure to vary inside the channel.

We then integrate (6) over y. Denoting s as the channel width, $\tilde{P} = \int_0^s P dy$, $V_x = \int_0^s v_x dy$. Taking into account $v_y\big|_{y=0,s} = 0$, (6) results in the following:

$$\frac{\partial V_x}{\partial x} = 0 \tag{7}$$

Next, we consider equation (5) and integrate it over x and over y. Denoting $\Delta P = P|_{\frac{l}{2}} - P|_{-\frac{l}{2}}$ as the pressure drop at the channel ends, $F_x = \int_{-l/2}^{l/2}\int_{-s/2}^{s/2} f_x dy\, dx$, . Then, equation (5) is written as:

$$\gamma l \frac{\partial^2 V_x}{\partial z^2} = F_x - \frac{s\Delta P}{\rho} \tag{8}$$

The solution for equation (8) is given by:

$$V_x = \frac{1}{\gamma l}\int_0^z d\tau_1 \int_0^{\tau_1} \left(F_x - \frac{s\Delta P}{\rho}\right) d\tau + Az + B \tag{9}$$

Under the conditions of adhesion to the channel walls at $z = 0$ and $z = d$, the solution is:

$$V_x = -\frac{1}{l\gamma}\left(\frac{z}{d}\int_0^d d\tau_1 \int_0^{\tau_1} \left(F_x - \frac{s\Delta P}{\rho}\right) d\tau - \int_0^z d\tau_1 \int_0^{\tau_1} \left(F_x - \frac{s\Delta P}{\rho}\right) d\tau\right) \tag{10}$$

To describe the random forces acting on the liquid, we use the following approach [26]. Assuming the force $f(x,y,z)$ can be described by a sum of derivatives of the stress tensor with respect to the spatial coordinates:

$$f(x,y,z) = \frac{\partial s_{xz}}{\partial z} + \frac{\partial s_{xy}}{\partial y} + \frac{\partial s_{xx}}{\partial x}. \tag{11}$$

The tensors S_{xz}, S_{xy}, S_{xx} are uncorrelated together, and therefore, their contributions to the hydrodynamic velocity fluctuations can be regarded to be independent from each other. As discussed in [25], the first summand in (11) dominates in thin channels and the other terms can be removed from consideration. Putting (11) in (5), one obtains:

$$V_x = -\frac{1}{l\gamma}\left(\frac{z}{d}\int_0^d \sigma_{xz}(\tau)d\tau - \int_0^z \sigma_{xz}(\tau)d\tau + \frac{zs\Delta P}{2\rho}(z-d)\right) \qquad (12)$$

where $\sigma_{xz} = \int_{-l/2}^{l/2}\int_{-s/2}^{s/2} S_{xz}\,dydx$. We require (12) to be solved under the condition of the absence of integral liquid flow in the channel. For this, one considers the average speed over a cross section $\overline{V} = 0$ and finds ΔP under this condition. The resulting equation is given below:

$$V_x = \frac{1}{l\gamma}\left(\left(\frac{3z^2}{d^2} - \frac{2z}{d}\right)\int_0^d \sigma_{xz}(\tau)d\tau - \frac{6z}{d^3}(z-d)\int_0^d d\tau\int_0^\tau \sigma_{xz}(\tau_1)d\tau_1 - \int_0^z \sigma_{xz}(\tau)d\tau\right) \qquad (13)$$

We consider the velocities at two points z and z_1. For the correlation of the random velocities $\langle V_x(z,\omega)V_x(z_1,-\omega)\rangle$, we use [27]:

‘

$$\langle S_{xz}(x,y,\tau_1,\omega)S_{xz}(x_1,y_1,\tau_2,-\omega)\rangle = 2\gamma\rho T\delta(x-x_1)\delta(y-y_1)\delta(z-z_1) \qquad (14)$$

The correlation functions $\langle\sigma_{xz}(\tau)\sigma_{xz}(\tau_1)\rangle$ are calculated to be:

$$\langle\sigma_{xy}(\tau)\sigma_{xy}(\tau_1)\rangle = \int_{-L/2}^{L/2} dx \int_{-L/2}^{L/2} dx_1 \int_{-S/2}^{S/2} dy \int_{-S/2}^{S/2} \langle S_{xz}(x,y,z,\omega)S_{xz}(x_1,y_1,z_1,-\omega)\rangle dy_1 \qquad (15)$$

After integrating (13) were the following:

$$\langle V_x(z,\omega)V_x(z_1,-\omega)\rangle_x = \begin{cases} \frac{2\rho Ts}{\gamma}\left[z - \frac{4zz_1}{d} + \frac{3z^2z_1}{d^2} + \frac{3zz_1^2}{d^2} - \frac{3z^2z_1^2}{d^3}\right], z < z_1 \\ \frac{2\rho Ts}{\gamma}\left[z_1 - \frac{4zz_1}{d} + \frac{3z^2z_1}{d^2} + \frac{3zz_1^2}{d^2} - \frac{3z^2z_1^2}{d^3}\right], z > z_1 \end{cases} \qquad (16)$$

Next, we consider the convective diffusion equation. Assuming that the hydrodynamic velocity is small, the solution to the convective diffusion equation (3) is found to be:

$$c = c_0 + c_{st} + c_1 \qquad (17)$$

where c_0 is the equilibrium concentration of the active component, c_{st} is the concentration in the stagnant electrolyte, and c_1 denotes changes in the concentration linear in hydrodynamic velocity.

Considering only the terms that do not depend on the velocity and those that are linear in velocity after a Fourier transform of the first equation in (3) on the x coordinate, we obtains the following system.

$$\begin{aligned}
&\frac{\partial^2 c_{st}}{\partial z^2} - k^2 c_{st} = 0 \\
&\frac{\partial^2 c_1}{\partial z^2} - (k^2 + \frac{i\omega}{D})c_1 = L(k,z) \\
&L(k,z) = \frac{ikc_{st}(k,z)}{D} V_x(z)
\end{aligned} \tag{18}$$

The solution of (18) can be expressed as follows:

$$\begin{aligned}
&c_{st}(k,z) = \frac{e^{-|k|z} + e^{-|k|(2d-z)}}{1 - e^{-2|k|d}} \frac{j_0(k)}{2Dq|k|} \\
&c_1(k,z) = \frac{j_1(k)}{2Dq\kappa} \frac{e^{\lambda z} + e^{2\lambda d - \lambda z}}{e^{2\lambda d} - 1} + \frac{1}{\kappa}\int_0^z L(\mathrm{k},\zeta)\sinh(\lambda z - \lambda\zeta)d\zeta - \\
&\quad - \frac{e^{\lambda z} + e^{-\lambda z}}{2\lambda \sinh(\lambda d)} \int_0^d L(\mathrm{k},\zeta)\cosh(\lambda d - \lambda\zeta)d\zeta
\end{aligned} \tag{19}$$

where $\kappa_k{}^2 = \mathrm{k}^2 - \frac{\mathrm{i}\omega}{\mathrm{D}}, \mathrm{Re}\kappa > 0$. $j_{0,1}(k) = \frac{1}{2\pi}\int_{S_{el}} j_{0,1}(\xi)e^{-ik\xi}d\xi$ is the Fourier transform of the electrical current density on the surface $z = 0$. Index S_{el} below the integral sign indicates integration over the electrode surface. We use the second and third equations for the boundary conditions (4) to find the unknown $j_{0,1}(\xi)$. This is done by entering $z = 0$ in (19) and carrying out an inverse Fourier confirmation. The result is given by the following set of integral equations:

$$\begin{aligned}
&0 = \frac{1}{4\pi Dq}\int_{-\infty}^{+\infty} dk \int_{S_{el}} \frac{e^{-|k|z} + e^{-|k|(2d-z)}}{1 - e^{-2|k|d}} \frac{j_0(\xi)}{2Dq|k|} e^{ik(\xi - x)}dx, \qquad x \in cathode \\
&c_a = \frac{1}{4\pi Dq}\int_{-\infty}^{+\infty} dk \int_{S_{el}} \frac{e^{-|k|z} + e^{-|k|(2d-z)}}{1 - e^{-2|k|d}} \frac{j_0(\xi)}{2Dq|k|} e^{ik(\xi - x)}dx, \qquad x \in anode \\
&0 = \frac{1}{4\pi Dq}\int_{-\infty}^{+\infty} dk \int_{S_{el}} \frac{j_1(\xi)}{\lambda} \frac{\cosh(\lambda d)}{\sinh(\lambda d)} e^{ik(x-\xi)}dk - \\
&- \int_{-\infty}^{+\infty} dk \frac{e^{ikx}}{\lambda \sinh(\lambda d)} \int_0^d L(\mathrm{k},\zeta)\cosh(\lambda d - \lambda\zeta)d\zeta , \quad x \in cathode \text{ and } x \in anode
\end{aligned} \tag{20}$$

In general, equation (20) can be solved using only numerical methods. To simplify the mathematical formulation, we assume that the electrical current density over the electrodes is uniform. This assumption is valid if the other characteristic sizes of the system (channel width, distance between electrodes, diffusion length) are larger than the electrode size. Otherwise, this can be considered to be a qualitative approximation. Under this assumption:

$$\begin{aligned}
&j_{0,1}(k) = \frac{\sin kb/2}{k\pi} \times \\
&\times\left(j_{0,1}(-3\mathrm{a})e^{-3ika} + j_{0,1}(-\mathrm{a})e^{-ika} + j_{0,1}(\mathrm{a})e^{ika} + j_{0,1}(3\mathrm{a})e^{3ika} \right)
\end{aligned} \tag{21}$$

Substituting this equation into (20) results in the following equations:

$$j_0(-3\mathrm{a}) = j_0(3\mathrm{a}) = -j_0(-\mathrm{a}) = -j_0(\mathrm{a}) \equiv j_0$$

$$j_1(3\mathrm{a}) = -j_1(3\mathrm{a}) = -j_1(-\mathrm{a}) = j_{0,1}(\mathrm{a}) \equiv j_1$$

$$j_0 = \frac{4Dq\pi c_0}{I}$$

$$j_1 = \frac{2j_0}{DI_1}\int_0^\infty dk\,\frac{\sin kb/2\cdot\sin 2ka\cdot\sin^2 ka}{\lambda k\sinh kd\sinh\lambda d}\int_0^d V_x(\zeta)\cosh(\mathrm{kd}-\mathrm{k}\zeta)\cosh(\lambda\,\mathrm{d}-\lambda\zeta)\,\mathrm{d}\,\zeta \qquad (22)$$

$$I = \int_0^\infty \frac{\cosh(kd)}{\sinh(kd)}\frac{\sin\left(kb/2\right)\sin^2 2ka}{k^2}\,dk$$

$$I_1 = \int_0^\infty \frac{\cosh(\lambda d)}{\sinh(\lambda d)}\frac{\sin\left(kb/2\right)\sin^2 2ka}{\lambda k}\,dk$$

Then, the power spectral density for the electrical current fluctuations due to the random hydrodynamic flow is given by the following equations.

$$\left\langle I_\omega^2\right\rangle = \frac{4j_0^2b^2}{D^2\left|I_1\right|^2}\int_0^\infty dk\,\frac{\sin kb/2\cdot\sin 2ka\cdot\sin^2 ka}{\lambda k\sinh kd\sinh\lambda d}\times$$
$$\times\int_0^\infty dk_1\,\frac{\sin k_1b/2\cdot\sin 2k_1a\cdot\sin^2 k_1a}{\lambda_1k_1\sinh k_1d\sinh\lambda_1d}\int_0^d d\zeta\int_0^d \mathrm{d}\,\zeta_1\left\langle V_x(z,\omega)V_x(z_1,-\omega)\right\rangle\times \qquad (23)$$
$$\times\cosh(\mathrm{kd}-\mathrm{k}\,\zeta)\cosh(k_1d-k_1\zeta)\cosh(\lambda d-\lambda\zeta)\cosh(\lambda_1d-\lambda_1\zeta)$$

After substituting into (16) and integrating over ζ and ζ_1, equation (23) results in the following formulae:

$$\left\langle I_\omega^2\right\rangle = \frac{2\rho TSj_0^2b^2}{D^2\left|I_1\right|^2\gamma}\int_0^\infty dk\,\frac{\sin kb/2\cdot\sin 2ka\cdot\sin^2 ka}{\lambda k\sinh kd\sinh\lambda d}\times$$
$$\times\int_0^\infty dk_1\,\frac{\sin k_1b/2\cdot\sin 2k_1a\cdot\sin^2 k_1a}{\lambda_1k_1\sinh k_1d\sinh\lambda_1d}[G(p,p_1)+G(p,\mathrm{r}_1)+G(\mathrm{r},p_1)+G(\mathrm{r},\mathrm{r}_1)-$$
$$-\frac{4}{d}(\mathrm{f(p)}+\mathrm{f(r)})(\mathrm{f(p_1)}+\mathrm{f(r_1)})+ \qquad (24)$$
$$+\frac{3}{d^2}\left[(\mathrm{g(p)}+g(\mathrm{r}))(\mathrm{f(p_1)}+\mathrm{f(r_1)})+(\mathrm{f(p)}+\mathrm{f(r)})(\mathrm{g(p_1)}+g(\mathrm{r_1}))\right]-$$
$$-\frac{3}{d^3}(\mathrm{g(p)}+g(\mathrm{r}))(\mathrm{g(p_1)}+g(\mathrm{r_1}))]$$

The following designations are used for simplicity:

$$
\begin{aligned}
p &= k + \lambda \\
p_1 &= k_1 + \lambda_1 \\
r &= \lambda - k \\
r_1 &= \lambda_1 - k_1 \\
G(x, \mathrm{y}) &= \frac{\sinh(\mathrm{xd}+\mathrm{yd})}{xy(x+y)} - \frac{\sinh(\mathrm{xd}-\mathrm{yd})}{xy(x-y)} \\
f(x) &= \left(\cosh(\mathrm{xd}) - 1\right)\big/ x^2 \\
g(x) &= 2\left(\sinh(\mathrm{xd}) - \mathrm{xd}\right)\big/ x^3
\end{aligned}
\tag{25}
$$

3. RESULTS AND DISCUSSION

Note that at high frequencies $p, p_1, r, r_1, \lambda, \lambda_1 \approx \sqrt{i\omega/D}$ and the current noise spectral density $\langle I_\omega^2 \rangle$ is approximated by $\sim\omega^{-1.5}$ behavior:

$$
\langle I_\omega^2 \rangle = \frac{8\sqrt{2}\rho T s j_0^2 b^2}{\gamma\sqrt{D\omega^3}} \left(\frac{\int_0^\infty \frac{\sin kb/2 \ \sin 2ka \ \sin^2 ka}{k \ \sinh kd} dk}{\int_0^\infty \frac{\sin kb/2 \ \sin^2 2ka}{k} dk} \right)^2 \tag{26}
$$

Another limit is $\omega \to 0$; i.e., the noise power spectral density $\langle I_\omega^2 \rangle$ does not depend on the frequency:

$$
\begin{aligned}
&\langle I_\omega^2 \rangle \\
&= \frac{2\rho T s j_0^2 b^2}{\gamma D^2 |I_1^2|} \int_0^\infty dk \frac{\sin kb/2 \ \sin 2ka \ \sin^2 ka}{k^2 \ \sinh^2 kd} \int_0^\infty dk_1 \frac{\sin k_1 b/2 \ \sin 2k_1 a \ \sin^2 k_1 a}{{k_1}^2 \ \sinh^2 k_1 d} \times \\
&\times \left[\frac{\sinh 2(k+k_1)d}{2kk_1(k+k_1)} - \frac{\sinh 2(k-k_1)d}{2kk_1(k-k_1)} + \frac{d}{2k^2}\left(\cosh 2kd - \frac{\sinh 2kd}{2kd}\right) \right. \\
&+ \frac{d}{2{k_1}^2}\left(\cosh 2k_1 d - \frac{\sinh 2k_1 d}{2k_1 d}\right) + \frac{2d^3}{3} \\
&- d^3 \left(\frac{\cosh 2kd - 1}{2k^2 d^2} + 1\right)\left(\frac{\cosh 2k_1 d - 1}{2{k_1}^2 d^2} + 1\right) \\
&+ \frac{d^3}{2}\left(\frac{\cosh 2kd - 1}{2k^2 d^2} + 1\right)\left(3\frac{\sinh 2k_1 d - 2k_1 d}{2{k_1}^2 d^2} + 1\right) \\
&+ \frac{d^3}{2}\left(\frac{\cosh 2k_1 d - 1}{2{k_1}^2 d^2} + 1\right)\left(3\frac{\sinh 2kd - 2kd}{2k^2 d^2} + 1\right) \\
&\left. - \frac{d^3}{3}\left(3\frac{\sinh 2k_1 d - 2k_1 d}{2{k_1}^2 d^2} + 1\right)\left(3\frac{\sinh 2kd - 2kd}{2k^2 d^2} + 1\right) \right]
\end{aligned}
\tag{27}
$$

For other frequencies, the integrals in (22) - (24) are calculated numerically. Figure 2 shows the result of the calculation for several sets of system parameters: $d/a = 1, b/a = 0.2$ - curve 1,

$d/a = 1, b/a = 0.2$ - curve 2, $d/a = 0.2, b/a = 0.2$ - curve 3, and $d/a = 0.1, b/a = 0.1$ - curve 4. For each combination of parameters, $\sqrt{\langle I_\omega^2 \rangle}$ is normalized over its maximum value. The horizontal axis gives a non-dimensional frequency $\omega_n = 4\omega a^2/D$.

We compare the experimental data reported in different papers [12, 15, 16]. The noise for the ampoule-type transducer with interelectrode distances of 40 and 100 microns has been studied in [12] for frequencies below 20 Hz, corresponding to $\omega_n < 100$ and $\omega_n < 400$. For the tested samples, after removal of temperature drifts, the resulting noise spectral density is approximately flat at $\omega_n < 10$ before showing a decrease with increasing frequency. The theoretical curves (Figure 2) show similar behavior. It should be emphasized that the correspondence is fairly good for curves 3 and 4, while curves 1 and 2 are only flat at $\omega_n < 1$.

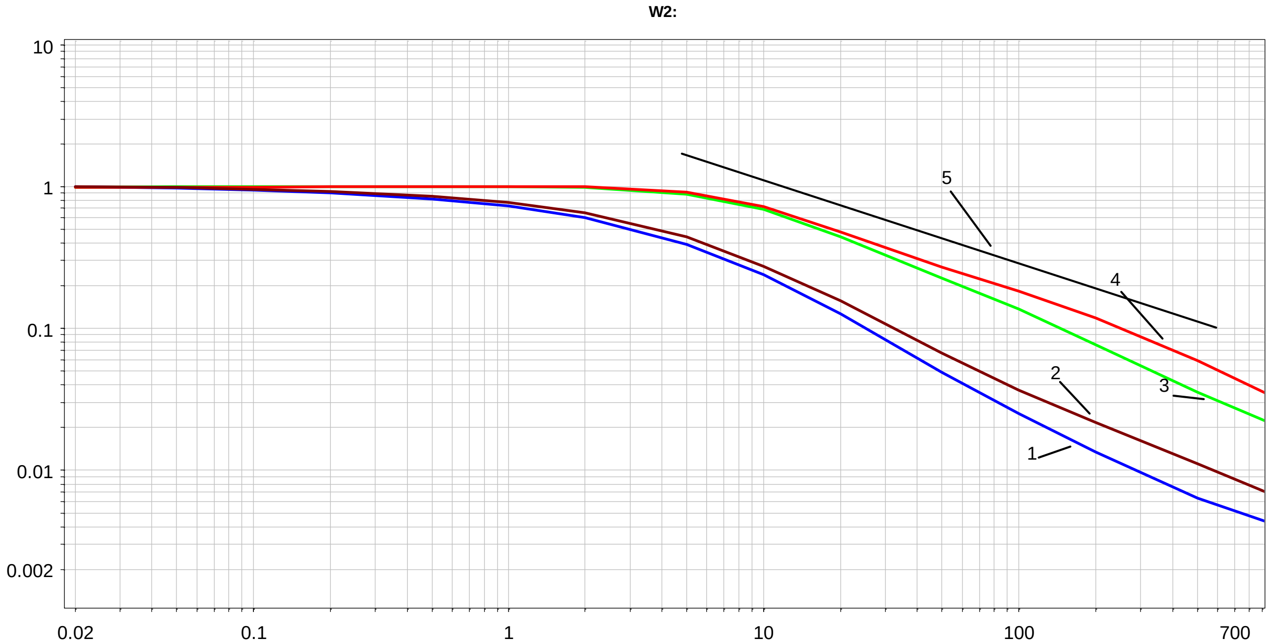

Figure 2. Normalized noise spectral density over its maximum value $\sqrt{\langle I_\omega^2 \rangle}$ calculated according to (22) - (24) vs the normalized frequency.

Legend: Curve 1 (blue) $d/a = 1, b/a = 0.2$, curve 2 (dark red) $d/a = 1, b/a = 0.2$, curve 3 (green) - $d/a = 0.2, b/a = 0.2$, and curve 4 (light red) $d/a = 0.1, b/a = 0.1$ - curve 4. Black line $\sim \omega^{-0.55}$ dependence.

Convective noise at higher frequencies has been previously studied in [15, 16, 13] and shown to have a $\sqrt{\langle I_\omega^2 \rangle} \sim \omega^{-\gamma}$ frequency behavior up to 100 Hz corresponding to $\omega_n \approx 500$, with $\gamma \geq 0.5$. The black line 5 in Figure 2 shows a $\sim \omega^{-0.55}$ dependence and lies parallel to curve 4, which approximately agrees with the behavior of curve 3 in the normalized frequency range from 10 to 100. Generally, at the very least, a qualitative correspondence is found between the modeling data and experimental curves.

4. CONCLUSIONS

The novelty of the presented results lies in the fact that they suggest, for the first time, a theoretical description for convective noise in the transducer of an electrochemical motion sensor. The model is based on the assumption that this noise is conditioned by the spatially non-uniform variation of hydrodynamic flow in the electrolyte, which is related to the influence of random local forces. Mathematically, the noise generating mechanism is described by the Navier-Stokes equation with a random term on the right-hand side.

The initial system of equations was reduced to integral equations to calculate the electric current density over the electrode surface – both steady and alternating, depending on the mechanical signal. The result of the calculations is a frequency dependence for the spectral power of the electric current fluctuations that is in correspondence with previously published experimental results.

ACKNOWLEDGEMENTS.
The results presented in this paper were obtained under the project supported by the Russian Ministry of Education and Science; the project ID is RFMEFI57817X0243.

References

1. A. T. J. Makris, J. Papoullia, *B. Geofis. Teor. Appl.*, 55 (2014) 561.
2. I. Koulakov, K. Jaxybulatov, N. M. Shapiro, I. Abkadyrov, E. Deev, A. Jakovlev, P. Kuznetsov, E. Gordeev, and V. Chebrov, *J. Volcanol. Geotherm. Res.*, 285 (2014) 36.
3. A. N. Antonov, A. S. Shabalina,A. Yu. Razin, S. Yu. Avdyukhina, I. V. Egorov, and V. M. Agafonov, *J. Atmos. Ocean. Tech.*, 34 (2017) 1743.
4. N. K. Kapustian, G. N. Antonovskaya, V. M. Agafonov, and K. A. Neumoin, in *6th European Workshop on theseismic behavior of Irregular and Complex Structures (6EWICS)*, 2011, 1.
5. V. A. Kozlov, V. M. Agafonov, J. Bindler, and A. V. Vishnyakov, *Proc. Inst. Navig. Natl. Tech. Meet.*, 2 (2006) 650.
6. E. V. Egorov, V.M. Agafonov, S. Yu. Avdyukhina, S. A. Borisov, *Sensors-Basel*, 18 (2018) 944.
7. D. Chen, G. Li, J. Wang, J. Chen, W. He, Y. Fan, T. Deng, and P. Wang, *Sensor. Actuat. A Phys.*, 202 (2013) 85.
8. H. Huang, V. Agafonov, and H. Yu, *Sensors-Basel*, 13 (2013) 4581.
9. Z. Sun, D. Chen, J. Chen, T. Deng, G. Li, and J. Wang, in *Proceedings of the IEEE International Conference on Micro Electro Mechanical Systems (MEMS)*, 2016 (2016).
10. B. M. Grafov, A. M. Kuznetsov, and A. E. Suntsov, *J. Electroanal. Chem.*, 533 (2002) 19–23
11. V. A. Kozlov and M. V Safonov, *Tech. Phys.*, 48 (2003) 1579.
12. V. M. Agafonov and D. L. Zaitsev, *Tech. Phys.*, 55 (2010) 130.
13. D. Zaitsev, V. Agafonov, E. Egorov, A. Antonov, and A. Shabalina, *Sensors-Basel*, 15 (2015) 29378.

14. G. Havskov, J., Alguacil, in *Instrumentation in Earthquake Seismology, Volume 22 of the series Modern Approaches in Geophysics*, (2010) 11.
15. E. V. Egorov, I. V. Egorov, and V. M. Agafonov, “Self-Noise of the MET Angular Motion Seismic Sensors,” *J. Sensors*, 2015 (2015), 512545.
16. I. V Egorov, A. S. Shabalina, and V. M. Agafonov, *IEEE Sens. J.*, 17 (2017) 2008.
17. M. Liang, H. Huang, V. Agafonov, R. Tang, R. Han, and H. Yu, in *Proceedings of the IEEE International Conference on Micro Electro Mechanical Systems (MEMS)*, 2016 (2016) 986.
18. Z. Sun, D. Chen, J. Chen, T. Deng, G. Li, and J. Wang, Procedia Engineer, 168 (2016) 247.
19. T. Deng, D. Chen, J. Chen, Z. Sun, G. Li, and J. Wang, *IEEE Sens. J.*, 16 (2016) 650.
20. Z. Sun, G. Li, L. Chen, J. Wang, D. Chen, and J. Chen, *2017 IEEE 12th Int. Conf. Nano/Micro Eng. Mol. Syst. NEMS 2017*, 1 (2017) 714.
21. V. M. Volgin and A. D. Davydov, *Russ. J. Electrochem.*, 48 (2012) 565.
22. V. Agafonov and E. Egorov, *Int. J. Electrochem. Sci.*, 11 (2016) 2205.
23. Z. Sun, V. Agafonov, and E. Egorov, *J. Electroanal. Chem.*, 661 (2011) 157.
24. G. Grün, K. Mecke, and M. Rauscher, *J. Stat. Phys.*, 122 (2006) 1261.
25. F. Detcheverry and L. Bocquet, *Phys. Rev. E.*, 88 (2013) 1–15
26. L. D. Landau and E. M. Lifshitz, *J. Exp. Theor. Phys.*, 32 (1957) 1957.
27. Landau L. D. and L. E. M., in *Statistical Physics Part 2*, Second., Pergamon Press, 1980, 397.